



# LUND UNIVERSITY

## Identification of triaxial strongly deformed bands in Hf-164

Marsh, J. C.; Ma, W. C.; Hagemann, G. B.; Janssens, R. V. F.; Bengtsson, Ragnar; Ryde, Hans; Carpenter, M. P.; Guerdal, G.; Hartley, D. J.; Hoffman, C. R.; Ijaz, Q. A.; Kondev, F. G.; Lauritsen, T.; Mukhopadhyay, S.; Riedinger, L. L.; Yadav, R. B.; Zhu, S.

*Published in:*

Physical Review C (Nuclear Physics)

*DOI:*

[10.1103/PhysRevC.88.041306](https://doi.org/10.1103/PhysRevC.88.041306)

2013

[Link to publication](#)

*Citation for published version (APA):*

Marsh, J. C., Ma, W. C., Hagemann, G. B., Janssens, R. V. F., Bengtsson, R., Ryde, H., Carpenter, M. P., Guerdal, G., Hartley, D. J., Hoffman, C. R., Ijaz, Q. A., Kondev, F. G., Lauritsen, T., Mukhopadhyay, S., Riedinger, L. L., Yadav, R. B., & Zhu, S. (2013). Identification of triaxial strongly deformed bands in Hf-164. *Physical Review C (Nuclear Physics)*, 88(4), Article 041306. <https://doi.org/10.1103/PhysRevC.88.041306>

*Total number of authors:*

17

### General rights

Unless other specific re-use rights are stated the following general rights apply:

Copyright and moral rights for the publications made accessible in the public portal are retained by the authors and/or other copyright owners and it is a condition of accessing publications that users recognise and abide by the legal requirements associated with these rights.

- Users may download and print one copy of any publication from the public portal for the purpose of private study or research.
- You may not further distribute the material or use it for any profit-making activity or commercial gain
- You may freely distribute the URL identifying the publication in the public portal

Read more about Creative commons licenses: <https://creativecommons.org/licenses/>

### Take down policy

If you believe that this document breaches copyright please contact us providing details, and we will remove access to the work immediately and investigate your claim.

LUND UNIVERSITY

PO Box 117  
221 00 Lund  
+46 46-222 00 00

## Identification of triaxial strongly deformed bands in $^{164}\text{Hf}$

J. C. Marsh,<sup>1</sup> W. C. Ma,<sup>1</sup> G. B. Hagemann,<sup>2</sup> R. V. F. Janssens,<sup>3</sup> R. Bengtsson,<sup>4</sup> H. Ryde,<sup>5</sup> M. P. Carpenter,<sup>3</sup> G. Gürdal,<sup>6</sup> D. J. Hartley,<sup>7</sup> C. R. Hoffman,<sup>3</sup> Q. A. Ijaz,<sup>1</sup> F. G. Kondev,<sup>6</sup> T. Lauritsen,<sup>3</sup> S. Mukhopadhyay,<sup>8</sup> L. L. Riedinger,<sup>9</sup> R. B. Yadav,<sup>1</sup> and S. Zhu<sup>3</sup>

<sup>1</sup>*Department of Physics and Astronomy, Mississippi State University, Mississippi State, Mississippi 39762, USA*

<sup>2</sup>*The Niels Bohr Institute, Blegdamsvej 17, DK-2100 Copenhagen, Denmark*

<sup>3</sup>*Physics Division, Argonne National Laboratory, Argonne, Illinois 60439, USA*

<sup>4</sup>*Department of Mathematical Physics, Lund Institute of Technology, S-221 00 Lund, Sweden*

<sup>5</sup>*Department of Nuclear Physics, Lund University, S-221 00 Lund, Sweden*

<sup>6</sup>*Nuclear Engineering Division, Argonne National Laboratory, Argonne, Illinois 60439, USA*

<sup>7</sup>*Department of Physics, United States Naval Academy, Annapolis, Maryland 21402, USA*

<sup>8</sup>*Nuclear Physics Division, Bhabha Atomic Research Centre, Mumbai 400085, India*

<sup>9</sup>*Department of Physics and Astronomy, University of Tennessee, Knoxville, Tennessee 37996, USA*

(Received 14 August 2013; published 28 October 2013)

Two new rotational bands of distinct character have been identified in  $^{164}\text{Hf}$ . They are suggested to correspond to the long-anticipated triaxial strongly deformed (TSD) bands predicted by theoretical studies. The bands have been linked to known states, and the level spins and energies could be determined. The bands are also substantially stronger in intensity and are located at lower spins than the previously observed TSD bands in  $^{168}\text{Hf}$ , hereby making  $^{164}\text{Hf}$  the best even-even system so far for the study of TSD structures in the  $A \sim 160$  mass region. Cranking calculations based on the modified-oscillator model suggest that the bands are associated with four-quasiparticle configurations that involve high- $j$  intruder ( $i_{13/2}$ )<sup>2</sup> proton orbitals.

DOI: [10.1103/PhysRevC.88.041306](https://doi.org/10.1103/PhysRevC.88.041306)

PACS number(s): 21.10.Re, 23.20.Lv, 27.70.+q

Considerable progress has been made over the past decade in the study of collective motion associated with a stable triaxial nuclear shape. In the  $A \sim 160$  mass region, families of rotational bands based on a wobbling excitation have been identified in  $^{163,165,167}\text{Lu}$  [1–4], possibly in  $^{161}\text{Lu}$  [5], and, more recently, in  $^{167}\text{Ta}_{94}$  [6]. Triaxial strongly deformed (TSD) bands based on quasiparticle excitations have also been observed in neighboring nuclei, such as  $^{164}\text{Lu}$  [7] and  $^{163}\text{Tm}_{94}$  [8]. These findings have been investigated extensively with different theoretical approaches—see, e.g., Refs. [8–12]. In some of the early studies, it was suggested that TSD minima associated with deformation parameters  $(\epsilon_2, \gamma) \sim (0.4, \pm 20^\circ)$  in the total energy surfaces are stabilized by large single-particle shell gaps present at proton numbers  $Z = 71$  and  $72$  and neutron numbers  $N = 94$  and  $97$  [13,14]. However, it has proved to be a considerable challenge to predict the behavior of TSD structures in specific nuclei in this region, even those that differ by only a single nucleon from the well-studied cases above.

Whereas, the observed TSD bands in the  $Z = 71$  Lu isotopes and  $N = 94$  isotones are consistent with the calculated TSD shell gaps, experimental searches in both  $^{166}\text{Hf}_{94}$  [15] and  $^{169}\text{Hf}_{97}$  [16] failed to uncover any TSD structure. Thus far, only two weak TSD bands were reported in  $^{168}\text{Hf}_{96}$  [17,18] but were not yet linked to the known normal deformed (ND) states. As a result, the presence of a significant  $Z = 72$  TSD shell gap seemed questionable. Furthermore, the occurrence of wobbling was first discussed for even-even nuclei [19].  $^{168}\text{Hf}$  is the only even-even isotope in the region which shows evidence for TSD structure. Neither of its TSD bands appear to result from a wobbling excitation, even though such motion was expected in some theoretical studies, see, e.g., Ref. [20]. Recently, the TSD bands in  $^{168}\text{Hf}$  were analyzed in detail

through calculations based on the configuration-constrained cranked Nilsson-Strutinsky model [21]. The latter further revealed that more high- $j$  intruder orbitals are involved in the  $^{168}\text{Hf}$  TSD bands than in the wobbling bands of the odd- $A$  Lu and Ta nuclei where a rotation aligned  $i_{13/2}$  quasiproton plays a crucial role, which allows wobbling to compete in energy with quasiparticle excitations.

In a comprehensive study of TSD structures in the  $A \sim 160$  region [22], Bengtsson determined that the yrast lines of the ND  $N = 92$  isotones are systematically higher in excitation energy at high spin than those of their neighbors. This may result in a lower relative excitation energy for the TSD bands that potentially leads to an increased population in fusion-evaporation residues. Thus,  $^{164}\text{Hf}_{92}$  could well be a better candidate to study TSD structures than  $^{166}\text{Hf}_{94}$  [22]. This effect, attributed to an elevated yrast line, seems to be supported by the stronger population of wobbling bands in  $^{163}\text{Lu}_{92}$  than in  $^{165}\text{Lu}_{94}$ .

Motivated by these considerations, an experimental study of  $^{164}\text{Hf}$  was undertaken. Here, we report on the identification of two bands with distinct characters, which are proposed to be the long-anticipated TSD bands in  $^{164}\text{Hf}$ . The bands have been linked to the known ND states, allowing the determination of the level spins, energies, and parities of the bands. This makes  $^{164}\text{Hf}$  the first even-even system in the mass region where a detailed comparison of the observed and calculated quantities for TSD bands could be performed. Furthermore, the bands cross the yrast line at spin 32 with relative intensities of  $\sim 2.9\%$  and  $\sim 1.6\%$ , respectively, as compared to an  $\sim 50\hbar$  crossing and an intensity of  $\sim 0.26\%$  for the band TSD1 in  $^{168}\text{Hf}$ . Eight ND bands in  $^{164}\text{Hf}$  have also been extended to high spins; they will be presented in a forthcoming paper.

High-spin states in  $^{164}\text{Hf}$  were populated through the  $^{94}\text{Zr}(^{74}\text{Ge}, 4n)$  reaction with a beam energy of 330 MeV at the ATLAS facility at Argonne National Laboratory. The target consisted of a self-supporting thin foil ( $\sim 0.76 \text{ mg/cm}^2$ ) of isotopically enriched  $^{94}\text{Zr}$ . Coincident  $\gamma$  rays were measured using the Gammasphere array [23], which consisted of 99 Compton-suppressed Ge detectors at the time of this experiment. A total of  $3.3 \times 10^9$  fourfold, or higher, prompt coincidence events was collected. In the off-line analysis, the data were sorted into a database where the  $\gamma$ -ray energies and detector identification were stored for each event. The RADWARE software package [24] was used to construct three-dimensional (cube) and four-dimensional (hypercube) histograms and to analyze the  $\gamma$ -ray coincidence relationships. The RADWARE band search routine was used extensively to look for weak bands. In addition, an analysis of so-called DCO ratios ( $\gamma$ -ray directional correlation from oriented nuclei [25]) was performed to determine the multipolarity of the  $\gamma$  rays; see Ref. [26] for more details on the technique. The spin and parity of the levels were then assigned based on the measured  $\gamma$ -ray multiplicities.

A partial level scheme of  $^{164}\text{Hf}$  from this study is presented in Fig. 1, and representative spectra for bands TSD1 and TSD2 can be found in Fig. 2. Previously, the ground-state band (GSB) and the two negative-parity bands AE and AF were observed up to the  $28^+$ ,  $31^-$ , and  $30^-$  levels, respectively [27,28]. The letter A in the band labels denotes the  $\nu i_{13/2}$  orbital, and the letter E (F) corresponds to the positive (negative) signature of the lowest negative-parity neutron orbital. Band AG was observed in this Rapid Communication for the first time and was assigned negative parity and odd spins based on the measured  $E2$  nature of both the band members and the 885- and 603-keV depopulating transitions to band AE. Band TSD1 mainly feeds band AG at the  $27^-$  level and is linked to band AE by two other  $\gamma$  rays. The relative intensities of the 824-, 872-, and 1006-keV decay-out transitions are  $2.5 \pm 0.3\%$ ,  $0.3 \pm 0.1\%$ , and  $0.5 \pm 0.2\%$ , respectively, of the total intensity feeding the ground state of  $^{164}\text{Hf}$ . The DCO ratios of the 824-keV  $\gamma$  ray and of all the in-band transitions between  $29^-$  and  $39^-$  in TSD1 are consistent with a stretched- $E2$  nature. Thus, negative parity and odd spins have been assigned to TSD1. Band TSD2 feeds the  $30^-$  and  $32^-$  states in band AF. The DCO ratios of the 975-keV  $\gamma$  ray and of the lowest three band members indicate that these transitions are of stretched-quadrupole character. Consequently, the band has been assigned negative parity and even spins. The relative intensity of the 932-keV  $\gamma$  ray, the strongest transition in band TSD2, is  $1.6 \pm 0.7\%$ .

The aligned angular momenta of the bands of interest are depicted in Fig. 3(a). As discussed in previous papers [27,28], the GSB undergoes the lowest  $i_{13/2}$  neutron band crossing (AB crossing) around  $\hbar\omega \sim 260$  keV. Bands AE and AF, the lowest negative-parity signature-partner bands, undergo the second lowest  $i_{13/2}$  neutron band crossing (BC crossing) at  $\hbar\omega \sim 320$  keV. The initial alignments of the TSD bands  $\sim 21\hbar$  are much larger than those of the ND bands. Furthermore, these bands do not exhibit the proton alignments seen in the ND bands at  $\hbar\omega \sim 500$  keV, which indicates that the high- $j$  intruder proton orbitals are already occupied at lower rotational

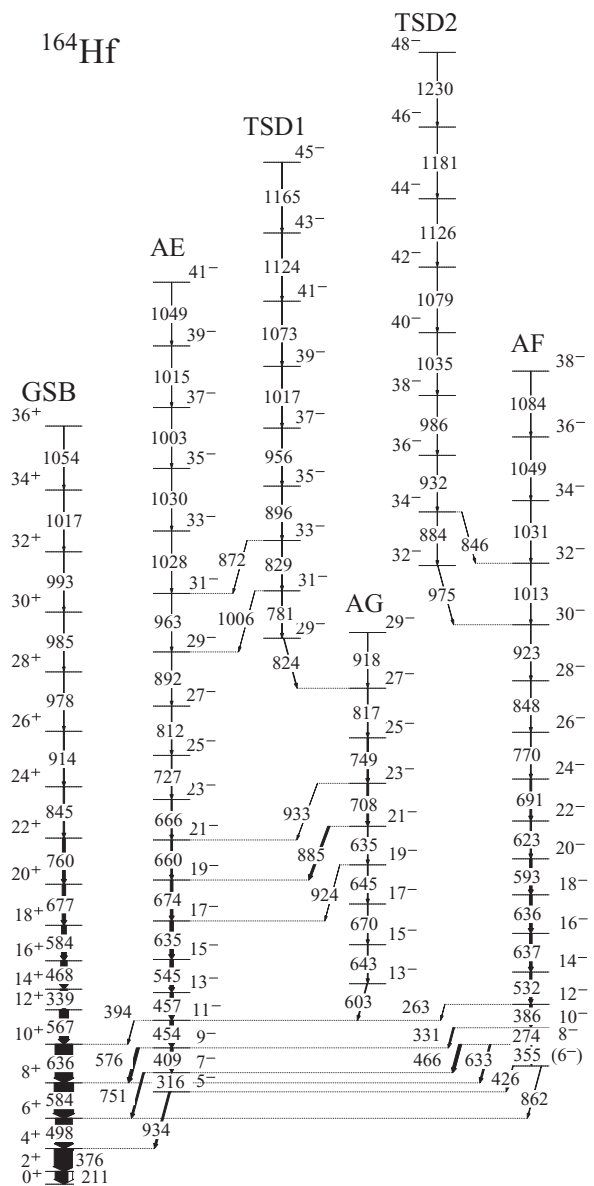


FIG. 1. Partial level scheme of  $^{164}\text{Hf}$  from this Rapid Communication. The arrow widths are proportional to the relative intensities of the  $\gamma$  rays. Transition energies are given in keV.

frequencies in the TSD sequences. Therefore, bands TSD1 and TSD2 are not associated with the ND structures. In addition, the average values of the dynamical moments of inertia  $J^{(2)}$  of the TSD bands are  $\sim 35\%$  higher than that of the ND band AF, as can be seen in Fig. 3(b), which indicates that the TSD bands have larger deformation than the ND band. The  $J^{(2)}$  values are close to those of the TSD bands in  $^{168}\text{Hf}$  where the transition quadrupole moment of band TSD1 has been measured to be  $Q_t \approx 11.4 \text{ e b}$  [17], which is substantially larger than  $Q_t \approx 6.4 \text{ e b}$  for the ND yrast band [18].

Theoretical calculations were performed based on the cranked modified-oscillator model [29] with model parameters and computational details as described in Ref. [30]. The total energy surfaces (TESs) were constructed in lattices of  $10 \times 11$  deformation points that cover a region of the  $(\epsilon, \gamma)$

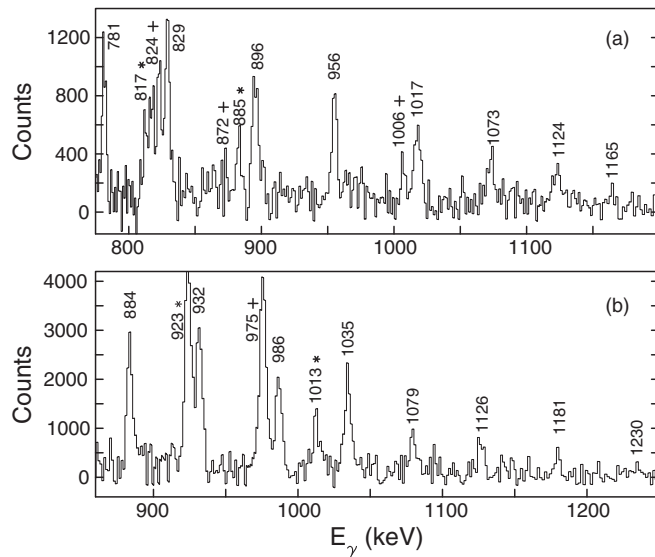


FIG. 2. Coincidence spectra of bands (a) TSD1 and (b) TSD2. The spectrum for TSD1 is a sum of double gates on all band members. The spectrum of TSD2 is a sum of double gates between the band members and the transitions in band AF. The symbols “+” and “\*” denote the decay-out transitions that link TSD and ND bands and the lower-spin transitions in other ND bands, respectively.

plane, which includes both normal and representative TSD deformations as illustrated in Fig. 4. At each lattice point, six values of the hexadecapole deformation  $\varepsilon_4$  were considered, and the total energy was minimized with respect to  $\varepsilon_4$ . The rotational frequency was varied in steps of 0.05 MeV from 0.0 MeV up to about 0.75 MeV. This is sufficient to ensure that the TESs can be constructed for angular momenta up to  $50\hbar$ . Pairing was included by assuming a constant pairing gap equal to 80% of the BCS value at zero rotational frequency for both protons and neutrons. Consequently, the gap used depends on the deformation but not on the rotational frequency. In the calculations, parity and signature are good quantum numbers, herewith enabling the labeling of theoretical configurations as  $P(\pi_1, \alpha_1)N(\pi_2, \alpha_2)$ . For protons,  $\pi_1 = 0$  (or 1), which indicates positive (or negative) parity and  $\alpha_1 = (\text{signature} \times 2)$ . The  $\pi_2$  and  $\alpha_2$  quantum numbers are defined similarly for neutrons. In total, there are 16 unique combinations of the parity and signature quantum numbers that allow the definition of 16 different parity-signature groups, each of which may contain several quasiparticle configurations.

In a first step, the energetically lowest configuration within each of the 16 parity-signature combinations was identified at each deformation point. TESs were then constructed by using the energies of these configurations. For a given parity-signature combination, excited configurations are only found if they are associated with a different deformation than the lowest one. These will then appear as coexisting energy minima in the TESs; the TSD bands that coexist with the ND ones were found with this approach.

The energies of the TSD bands for all 16 parity-signature combinations were calculated. For most of these, the energy of the TSD bands was found to be nearly the same. However, a few configurations stand out by being at lower excitation energy;

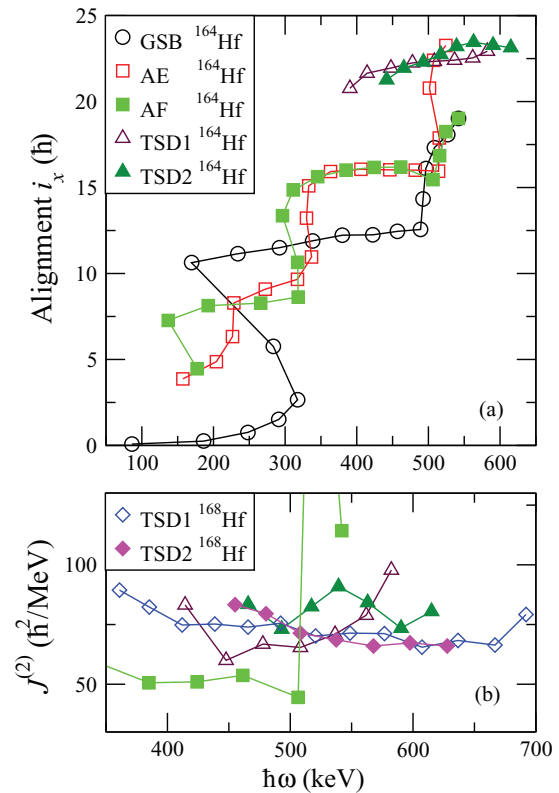


FIG. 3. (Color online) (a) Aligned angular momenta  $i_x$  and (b) dynamical moments of inertia  $J^{(2)}$  as functions of the rotational frequency  $\hbar\omega$  for bands in  $^{164}\text{Hf}$  and  $^{168}\text{Hf}$ . Harris parameters  $J_0 = 15\hbar^2/\text{MeV}$  and  $J_1 = 65\hbar^4/\text{MeV}^3$  were used to subtract the angular momentum of the rotating core.

see Fig. 5. A common feature for the latter configurations is that they have the same proton configuration  $P(0, 0)$ , which translates to  $\pi(i_{13/2})^2$ ; i.e., the same proton configuration as in the TSD bands in  $^{168}\text{Hf}$ . This is not surprising since both nuclei have the same  $Z = 72$  proton number. By assuming that the parity is negative, as determined experimentally, there are two low-lying theoretical configurations  $[P(0, 0)N(1, 2)$  and  $P(0, 0)N(1, 0)$  with odd and even spins, respectively], which may correspond to the observed TSD bands. These

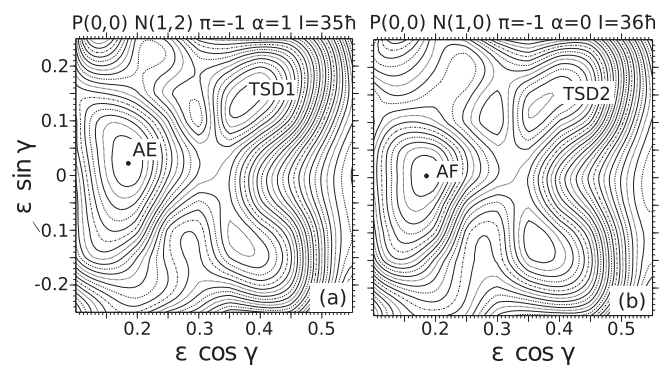


FIG. 4. Calculated TESs for the configurations (a)  $P(0, 0)N(1, 2)$  and (b)  $P(0, 0)N(1, 0)$  in  $^{164}\text{Hf}$ . The energy difference between the contour lines is 0.2 MeV. See text for details.

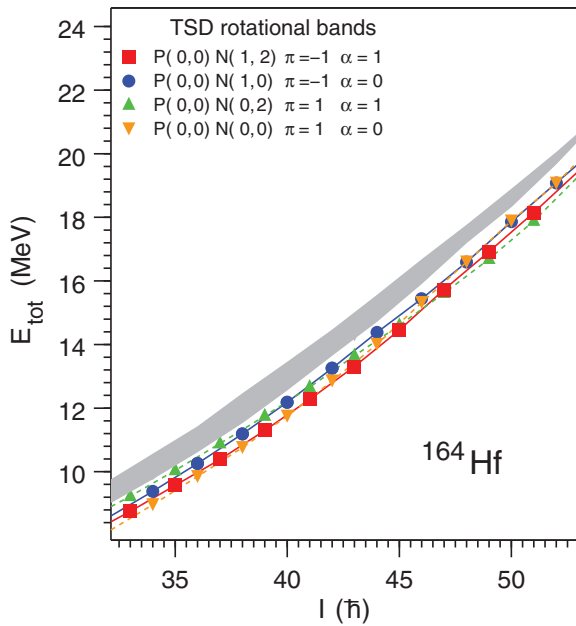


FIG. 5. (Color online) TSD rotational bands with the lowest energy in the different parity-signature groups. Only the four lowest bands are shown as individual ones. The lowest bands in the other parity-signature groups lie close together in the shaded region.

configurations contain two quasineutrons. The excited negative-parity neutron occupies an  $N = 5$  level dominated by components of  $\nu h_{9/2}$  parentage ( $\sim 65\%$ ). The excited positive-parity neutron is in an  $N = 6$  level ( $\nu i_{13/2}$ ) for the  $N(1, 0)$  configuration and in an  $N = 4$  level ( $\sim 30\%$   $\nu g_{7/2}$  occupation) for the  $N(1, 2)$  configuration. These are not the same as in  $^{168}\text{Hf}$  where a  $\nu j_{15/2}$  neutron level is occupied in the TSD bands [18]. Bands TSD1 and AE can be associated with coexisting energy minima in the lowest  $P(0, 0)N(1, 2)$  TES (Fig. 4, left panel); bands TSD2 and AF are represented by energy minima in the lowest  $P(0, 0)N(1, 0)$  TES (Fig. 4, right panel).

Figure 6 provides a comparison between calculated and observed rotational bands near the yrast line. The energy scale

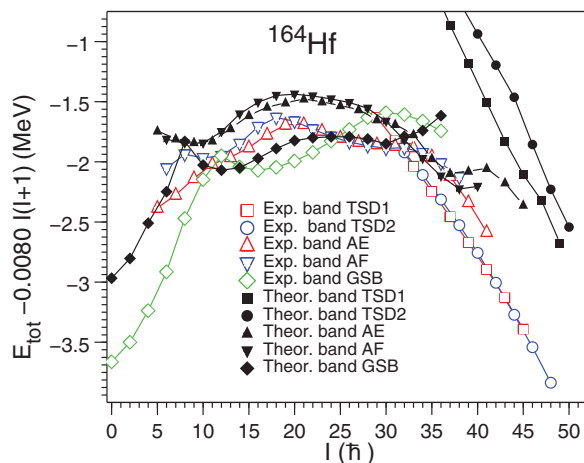


FIG. 6. (Color online) Experimental and calculated rotational band energies minus a rigid-rotor reference. The experimental bands are shifted downward by 3.66 MeV. See text for details.

is the one used in the calculations with the zero point that corresponds to a spherical nonrotating liquid drop energy. To facilitate the comparison, the data are shifted down by 3.66 MeV as this minimizes the difference in energy for levels between 14 and  $36\hbar$  in the GSB. This is the spin range where the reduced pairing gap (80% of the self-consistent value in the ground state) is most relevant. Both similarities and differences can be observed. Indeed, the main features in the calculations and the data are the same: The GSB forms the low-spin part of the yrast line. At higher spins, it is crossed by the negative-parity bands AE and AF. Finally, at the highest spins, the TSD bands come steeply down, both in the calculations and in the data. Some details also agree, such as the sharp AB crossing, clearly seen in the GSB. A reversed signature splitting between bands AE and AF, relative to that expected for the low-spin quasiparticle structure of orbitals E and F, is present in both the calculations and the data as well. The observed TSD bands are lower than the two calculated ones by  $\sim 1.4$  and  $\sim 1.8$  MeV around spin 40, but their slopes agree well. The value of the slope is closely related to the alignments and the kinematic moment of inertia, and this value is smaller here than that of the TSD bands in  $^{168}\text{Hf}$  (see Fig. 6 in Ref. [18]). The calculations suggest that the difference is caused by the role of the additional high- $j$  intruder orbital  $\nu j_{15/2}$ , involved in  $^{168}\text{Hf}$ .

The most important differences appear for the GSB before the AB crossing and for the TSD bands. In both cases, the calculated energies are too high. For the GSB, the difference is mainly caused by the reduced pairing gap used in the calculations, but for the TSD bands, the reason is less clear. The deformation dependence of the liquid drop energy could possibly play a role. Another disturbing difference for the TSD bands is the fact that the experimental bands essentially lie on top of each other, whereas, the calculated ones show a clear energy splitting. This splitting is a result of the way the theoretical TSD bands compared to the experimental ones were chosen. The theoretical bands are the lowest negative-parity bands with odd and even spins, respectively. These turn out to have different structures; the odd-spin band has a quasineutron in an  $N = 4$  level, whereas, the corresponding neutron occupies an  $N = 6$  level in the even-spin one. Levels from both of these shells are present near the Fermi surface at the TSD shapes. Their relative positions are not well known, and this, in turn, leads to an uncertainty in the relative position of the calculated TSD bands. Another strategy for finding theoretical counterparts to the experimental bands would be to search for odd- and even-spin negative-parity bands with little or no energy splitting. Such bands may exist since there are excited bands in the energetically favorable parity-signature groups that lie well below the shaded region of Fig. 5. A more systematic search for such bands than the one carried out in the present Rapid Communication may be necessary. Hence, the theoretically assigned configurations for the observed TSD bands remain uncertain. Figure 5 indicates that at least two TSD bands with positive parity are expected to lie on or very close to the yrast line at high spin, but no such bands have been observed. The reason for this observation is unclear. Furthermore, it will be difficult to observe collective wobbling excitations based on these TSD bands as many other TSD bands based on various quasiparticle

excitations are calculated to lie close to each other in excitation energy. Such a situation has been discussed in more detail in Ref. [31].

To summarize, two new bands of distinct character have been identified in  $^{164}\text{Hf}$  and have been linked to known states, which allows the determination of the level spins, energies, and parities of the bands. Based on their rotational properties and on comparisons with cranking calculations with a modified-oscillator potential, the bands are suggested to be the long-predicted TSD bands in  $^{164}\text{Hf}$ . Proposed configurations for the bands involve four quasiparticles, which include the high- $j$  intruder  $(i_{13/2})^2$  proton orbitals. Furthermore, the new bands

are substantially more intense and are observed at lower spins than the previously reported TSD bands in  $^{168}\text{Hf}$ , which makes  $^{164}\text{Hf}$  the best even-even system so far for the study of TSD structures in the  $A \sim 160$  mass region.

The authors thank the ANL operations at Gammasphere and gratefully acknowledge the efforts of J. P. Green for the target preparation. This work was supported by the U.S. Department of Energy, Office of Nuclear Physics, under Grants No. DE-FG02-95ER40939 (MSU) and No. DE-AC02-06CH11357 (ANL) and the National Science Foundation under Grant No. PHY-1203100 (USNA).

- 
- [1] S. Ødegård *et al.*, *Phys. Rev. Lett.* **86**, 5866 (2001).  
 [2] D. R. Jensen *et al.*, *Phys. Rev. Lett.* **89**, 142503 (2002).  
 [3] G. Schönwaßer *et al.*, *Phys. Lett. B* **552**, 9 (2003).  
 [4] H. Amro *et al.*, *Phys. Lett. B* **553**, 197 (2003).  
 [5] P. Bringel *et al.*, *Eur. Phys. J. A* **24**, 167 (2005).  
 [6] D. J. Hartley *et al.*, *Phys. Rev. C* **80**, 041304(R) (2009).  
 [7] P. Bringel *et al.*, *Phys. Rev. C* **75**, 044306 (2007).  
 [8] N. S. Pattabiraman *et al.*, *Phys. Lett. B* **647**, 243 (2007).  
 [9] I. Hamamoto and G. B. Hagemann, *Phys. Rev. C* **67**, 014319 (2003).  
 [10] Y. R. Shimizu, T. Shoji, and M. Matsuzaki, *Phys. Rev. C* **77**, 024319 (2008).  
 [11] B. G. Carlsson, *Intl. J. Mod. Phys. E* **16**, 634 (2007).  
 [12] K. Sugawara-Tanabe and K. Tanabe, *Phys. Rev. C* **82**, 051303(R) (2010).  
 [13] H. Schnack-Petersen *et al.*, *Nucl. Phys. A* **594**, 175 (1995).  
 [14] R. Bengtsson and H. Ryde, *Eur. Phys. J. A* **22**, 355 (2004).  
 [15] D. R. Jensen *et al.*, *Eur. Phys. J. A* **8**, 165 (2000).  
 [16] K. A. Schmidt *et al.*, *Eur. Phys. J. A* **12**, 15 (2001).  
 [17] H. Amro *et al.*, *Phys. Lett. B* **506**, 39 (2001).  
 [18] R. B. Yadav *et al.*, *Phys. Rev. C* **78**, 044316 (2008).  
 [19] A. Bohr and B. R. Mottelson, *Nuclear Structure* (Benjamin, New York, 1975), Vol. II.  
 [20] M. Matsuzaki, Y. R. Shimizu, and K. Matsuyanagi, *Phys. Rev. C* **69**, 034325 (2004).  
 [21] A. Kardan, I. Ragnarsson, H. Miri-Hakimabad, and L. Rafat-Motevali, *Phys. Rev. C* **86**, 014309 (2012).  
 [22] R. Bengtsson, [www.matfys.lth.se/staff/Ragnar.Bengtsson/TSD.html](http://www.matfys.lth.se/staff/Ragnar.Bengtsson/TSD.html)  
 [23] I. Y. Lee, *Nucl. Phys. A* **520**, 641 (1990).  
 [24] D. C. Radford, *Nucl. Instrum. Methods Phys. Res., Sect. A* **361**, 297 (1995).  
 [25] K. S. Krane, R. M. Steffen, and R. M. Wheeler, *Nucl. Data Tables* **11**, 351 (1973).  
 [26] R. B. Yadav *et al.*, *Phys. Rev. C* **80**, 064306 (2009).  
 [27] K. P. Blume *et al.*, *Nucl. Phys. A* **464**, 445 (1987).  
 [28] J. N. Mo *et al.*, *Nucl. Phys. A* **472**, 295 (1987).  
 [29] T. Bengtsson, *Nucl. Phys. A* **496**, 56 (1989).  
 [30] R. Bengtsson, T. Bengtsson, M. Bergström, H. Ryde, and G. B. Hagemann, *Nucl. Phys. A* **569**, 469 (1994).  
 [31] Y. C. Zhang *et al.*, *Phys. Rev. C* **76**, 064321 (2007).